Icarus 318 (2019) 241–250

Contents lists available at ScienceDirect

Icarus

journal homepage: www.elsevier.com/locate/icarus

Mineralogy of the Urvara–Yalode region on Ceres

A. Longobardo[a,*], A. Galiano[a], E. Ammannito[b], F.G. Carrozzo[a], M.C. De Sanctis[a], E. Palomba[a,c], F. Zambon[a], A. Frigeri[a], M. Ciarniello[a], A. Raponi[a], F. Tosi[a], M.T. Capria[a,c], K. Stephan[d], C.A. Raymond[e], C.T. Russell[f]

[a] INAF-IAPS, via Fosso del Cavaliere 100, I-00133 Rome, Italy
[b] ASI-URS, via del Politecnico snc, I-00133 Rome, Italy
[c] ASI-ASDC, via del Politecnico snc, I-00133 Rome, Italy
[d] Institute for Planetary Research, Deutsches Zentrum fur Luft- und Raumfahrt (DLR), D-12489 Berlin, Germany
[e] California Institute Technology JPL, 91109 Pasadena, CA, USA
[f] UCLA, 90095 Los Angeles, CA, USA

ARTICLE INFO

Article history:
Received 23 October 2017
Revised 22 November 2017
Accepted 7 December 2017
Available online 9 December 2017

Keywords:
Asteroid Ceres
Asteroids
Spectroscopy

ABSTRACT

We studied the distribution in the Urvara–Yalode region of Ceres (latitudes 21–66°S, longitudes 180–360°E) of main spectral parameters derived from the VIR imaging spectrometer onboard the NASA/Dawn spacecraft, as an overall study of Ceres mineralogy reported in this special issue. In particular, we analyzed the distribution of reflectance at 1.2 μm, band depth at 2.7 and 3.1 μm, ascribed to magnesium and ammoniated phyllosilicates, respectively.

Whereas the average band depths of this region are lower than eastern longitudes, reflecting the E-W dichotomy of abundance of phyllosilicates on Ceres, spectral variations inside this region are observed in the following units: (a) the central peak of the Urvara crater (45.9°S, 249.2°E, 170 km in diameter), showing a deep 3.1 μm band depth, indicating an ammonium enrichment; (b) the cratered terrain westwards of the Yalode basin (42.3°S, 293.6°E, 260 km in diameter), where absorption bands are deeper, probably due to absence of phyllosilicates depletion following the Yalode impact; (c) the hummocky cratered floor of Yalode and Besua (42.4°S, 300.2°E) craters, characterized by lower albedo and band depths, probably due to different roughness; (d) Consus (21°S 200°E) and Tawals (39.1°S, 238°E) craters, whose albedo and band depths decreasing could be associated to different grain size or abundance of dark materials. Twenty-two small scale (i.e., lower than 400 m) bright spots are observed: because their composition is similar to the Ceres average, a strong mixing may have occurred since their formation.

1. Introduction

NASA's Dawn mission has orbited (1) Ceres since March 2015 (Russell and Raymond, 2011), improving our knowledge of the dwarf planet. Dawn has taken color and imaging data by means of the Framing Camera (FC) (Sierks et al., 2011), spectra and hyperspectral images by means of the Visible and InfraRed mapping spectrometer (VIR) (De Sanctis et al., 2011), elemental maps by means of the Gamma Ray and Neutron Detector (GRaND) (Prettyman et al., 2011), as well as radio science data.

Ceres is a dark object, with an average reflectance at 30° phase of 0.03 at 0.55 μm (Ciarniello et al., 2017) and 0.75 μm (Longobardo et al., 2017). The spectroscopic analyses performed with the VIR instrument suggest an average composition of magnesium-rich and ammoniated phyllosilicates, magnesium carbonates and a dark material (De Sanctis et al., 2015): the absorption bands in reflectance spectra centered at 2.7 μm (hydration band of phyllosilicates), 3.1 μm (ammonium), 3.4 and 3.9 μm (mainly Mg-carbonates) have been detected across the entire surface (Ammannito et al., 2016).

However, some regions deviate from Ceres' average spectral behavior. Several bright spots, i.e. areas with an albedo at least 30% larger than their surroundings, have been detected on the Ceres surface (Stein et al., 2017; Palomba et al., 2017a). Whereas most of them show spectral signatures similar to the Ceres average, some bright spots are spectrally peculiar. In particular, the reflectance at 0.55 μm of Cerealia Facula and Vinalia Faculae, located inside the Occator crater (20°N 240°E), reaches values up to 0.26 (De Sanctis et al., 2016), and their spectra are characterized by a deepening and a longward shift of the 2.7, 3.4 and 3.9 μm

* Corresponding author.
E-mail address: andrea.longobardo@iaps.inaf.it (A. Longobardo).

https://doi.org/10.1016/j.icarus.2017.12.011
0019-1035/

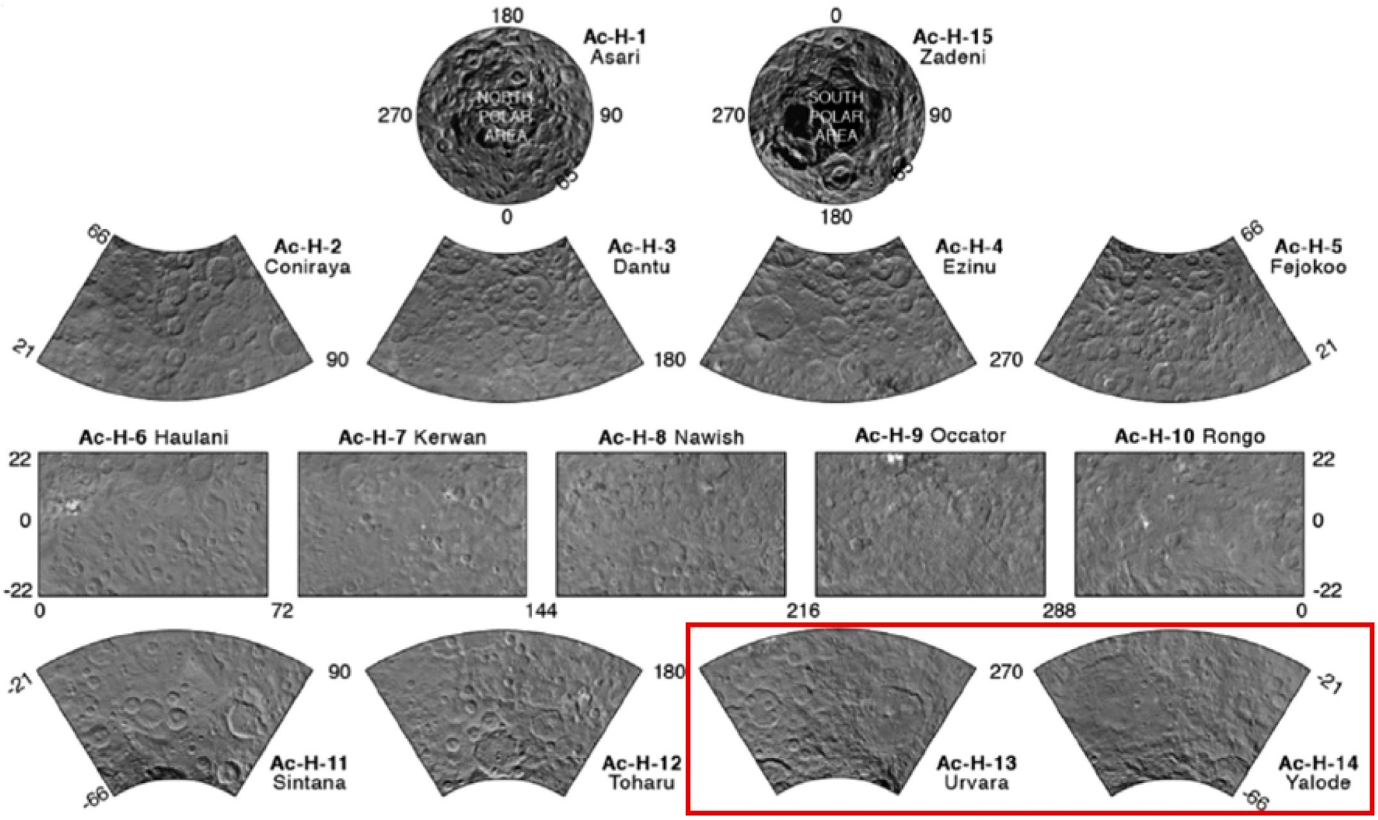

Fig. 1. Location of the Urvara and Yalode quadrangles on Ceres.

bands. These behaviors have been ascribed to a Na-carbonate enrichment and to occurrence of Al-phyllosilicates (instead of Mg-ones) (De Sanctis et al., 2016; Palomba et al., 2017a). Spectrophotometric behavior of the faculae suggests different physical properties of the regolith, such as grain size (Longobardo et al., 2017; Raponi et al., 2017a; Stephan et al., 2017). A few bright spots, when observed at low/intermediate ground resolution, show a spectral behavior intermediate between the Occator faculae and the Ceres average (e.g., Oxo crater, 43°N 360°E), suggesting a possible evolution of bright spots from the Occator family (the youngest features) to typical bright spots (Palomba et al., 2017a). In fact, detailed analysis of the carbonates distribution and composition indicate that most of the bright areas are comprised of Na-carbonate (Carrozzo et al., 2017a).

Other variations across the Ceres surface are indicated by the 3.4 μm band, consisting of an overlapping of absorptions due to different carriers. In this regard, the most peculiar region is Ernutet (52°N, 45°E), where the deepening of this band has been ascribed to the occurrence of organics (De Sanctis et al., 2017a).

The division of the Ceres surface into fifteen quadrangles has allowed more detailed study of the dwarf planet, characterizing also small-scale features, from both geological (Williams et al., 2017a) and mineralogical (McCord and Zambon, 2017) points of view.

This paper is focused on the spectral and mineralogical mapping of the Urvara and Yalode quadrangles, spanning longitudes from 180° to 270°E and from 270°E to 360°E, respectively, with both located at latitudes from 21°S to 66°S (Fig. 1).

The two quadrangles are named after their most prominent features, i.e., the Yalode (42.3°S, 293.6°E, 260 km in diameter) and Urvara (45.9°S, 249.2°E, 170 km in diameter) craters, the second and third largest basins on Ceres, respectively, after Kerwan (11°S, 124°E, 280 km in diameter, Williams et al. (2017b), Palomba et al. (2017b)). The Urvara crater is morphologically heterogeneous, characterized by a central peak, a terrace and smooth material, located in the southern and northern parts of the crater, respectively (Crown et al., 2017). The Yalode crater is instead more degraded and geologically uniform. Small craters are superimposed on these two basins, indicating more recent events, i.e., Tawals (39.1°S, 238°E) on the Urvara crater and Lono (36.7°S, 304.3°E) and Besua (42.4°S, 300.2°E) on Yalode (Crown et al., 2017). The Urvara and Yalode material and ejecta cover most of the quadrangles' area, except for the western region of the Urvara quadrangle (i.e., longitudes westwards than 210°E) and the eastern regions of the Yalode quadrangle (i.e., longitudes eastwards than 350°E), corresponding to old, cratered terrains (Crown et al., 2017). Several craters are found in these terrains: Consus (21°S, 200°E), Meanderi (40.9°S, 193.7°E) and Fluusa (31.5°S, 177.9°E) in the Urvara quadrangle, and Belun (33.7°S, 356.3°E), Mondamin (63.0°S, 353.6°E) and Tibong (29.8°S, 352.2°E) in the Yalode quadrangle. According to the geological evolution inferred by Crown et al. (2017), the cratered terrains formed first, then the Yalode and Urvara impact took place (1.1 Ga and 120–140 Ma ago, respectively, according to the lunar-derived model (Hiesinger et al., 2016)), followed by the small impact craters superimposed on the two basins.

From VIR data (Section 2), we extracted spectral parameters (Section 3) and built spectral maps (Section 4). The mineralogical analysis of the main features is discussed in Section 5, and conclusions are summarized in Section 6.

2. Data

The VIR imaging spectrometer is composed of an optical head, including a visible (0.2–1 μm, sampling 1.8 nm) and an infrared (1–5 μm, sampling 9.8 nm) channel (De Sanctis et al., 2011). The VIR products are hyperspectral images, i.e., bi-dimensional spatial

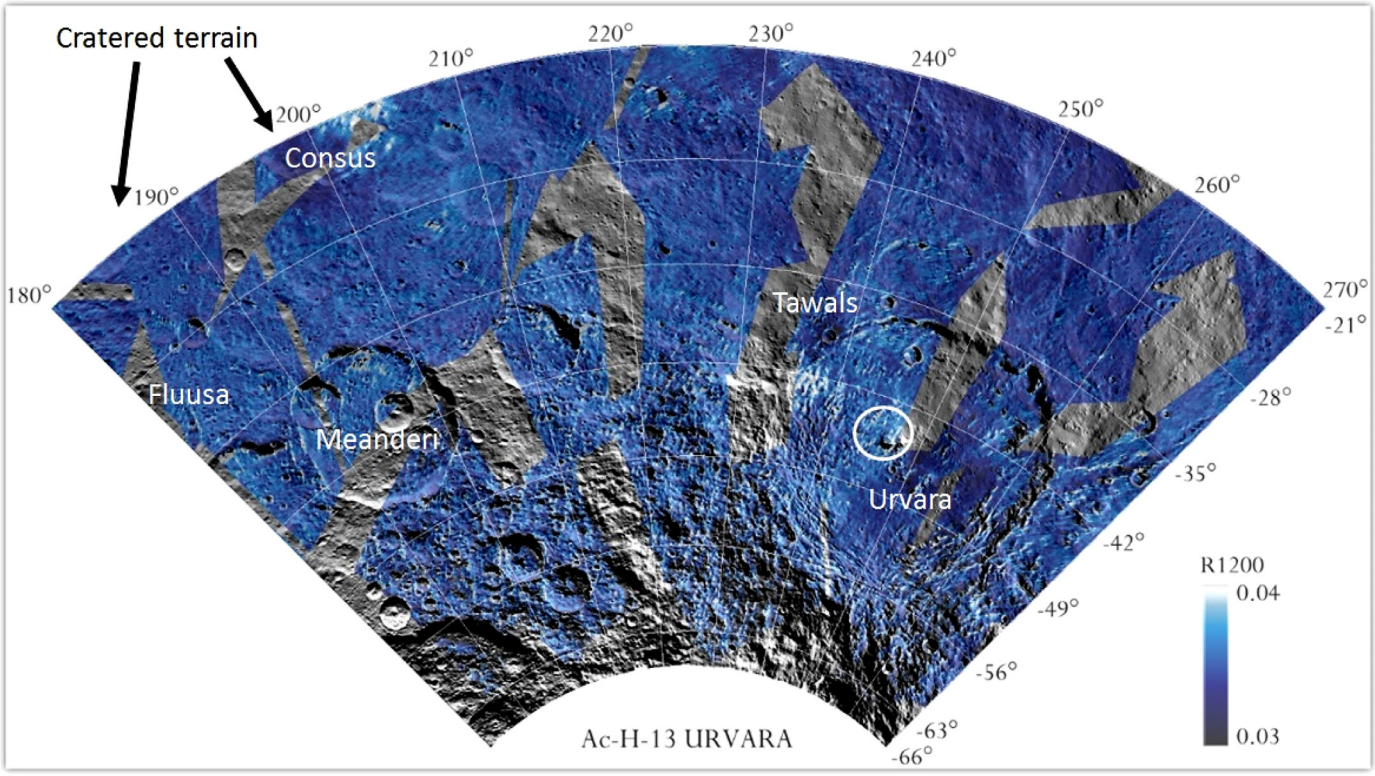

Fig. 2. Map of 1.2 μm reflectance at 30° phase of the Urvara quadrangle, superimposed on the Framing Camera (FC) mosaic with a transparence of 25%. Gray indicates no VIR coverage or excluded data. The white circle encloses the Urvara peak.

images acquired simultaneously at 864 wavelengths (432 per channel).

VIR spectra have been calibrated in radiance factor *I/F* (in the following, we will consider the terms radiance factor, *I/F* and reflectance as synonymous), according to the procedure by Filacchione and Ammannito (2014). Spectral artifacts were removed by building an artifact matrix, given by systematic spectral residuals with respect to the spectrum averaged on a single acquisition (Carrozzo et al., 2016). Spectra were then modeled as a sum of a reflected and thermally emitted signal, in order to remove the latter (Raponi et al., 2017b). Finally, the application of Hapke's model (Hapke, 2012) to VIR data (Ciarniello et al., 2017) allowed for obtaining photometrically corrected spectra.

Coherently with mineralogical mapping of other quadrangles, we considered VIR data acquired from a spacecraft altitude of ~1470 km during the High Altitude Mapping Orbit (HAMO), lasting from 17 August to 23 October 2015. These data guarantee both a good spatial coverage and spatial resolution (i.e. 360–400 m/pixel). We also studied the small-scale bright spots included in the two quadrangles, by means of high spatial resolution data (i.e. 90–110 m/pixel), acquired during the Low Altitude Mapping Orbit (LAMO) from a spacecraft altitude of ~385 km.

However, we do not have full coverage of the two quadrangles, because we removed from our dataset all observations acquired under incidence angles larger than 70°, where the influence of illumination conditions is not perfectly removed. Because the southern quadrangles are often observed under unfavorable illumination conditions, some areas cannot be analyzed, and in some cases residual photometric effects are observed even in the selected data.

3. Tools

The mineralogical analysis is based on reflectance at 1.2 μm, band depth at 2.7 μm and band depth at 3.1 μm, corrected at a phase angle of 30°. Band depths were calculated as $1 - R_c/R_{con}$, being R_c and R_{con} the measured reflectance and the continuum at the band center (i.e., the band minimum after the continuum removal) wavelength (Clark and Roush, 1984). Continua are defined as straight lines, as described in detail by Frigeri et al. (this issue). The centers of these bands do not vary in these quadrangles (and in general on the Ceres surface, except for a few locations), and for this reason, are not shown.

Band depths at 3.4 and 3.9 μm also have a uniform distribution on Ceres, except for some areas corresponding in most cases to bright spots and carbonate enrichments (Carrozzo et al., 2017b; Palomba et al., 2017a). We will discuss these cases for regions inside the Urvara and Yalode quadrangles.

4. Global maps

The Urvara quadrangle maps of reflectance at 1.2 μm, band depth at 2.7 μm, band depth at 3.1 μm and RGB color, where each color is associated to a spectral parameter, are shown in Figs. 2–5, respectively, whereas the same spectral parameters are mapped on the Yalode quadrangle in Figs. 6–9, respectively. All the maps are superimposed on the Framing Camera mosaic, and the main geological features of the quadrangles are highlighted.

An increasing North-South gradient of values of reflectance and band depth at 3.1 μm is observed, due to residuals of photometric correction. For this reason, we do not compare values of these spectral parameters with equatorial and Northern quadrangles, but only among the Southern quadrangles (i.e. Sintana, Toharu, Urvara and Yalode) observed at very similar illumination conditions.

Whereas reflectance does not show variations from western (Sintana and Toharu) to eastern (Urvara and Yalode), the two absorption bands are, on average, deeper on the western quadrangles (De Sanctis et al., 2017b). The same east-west dichotomy is

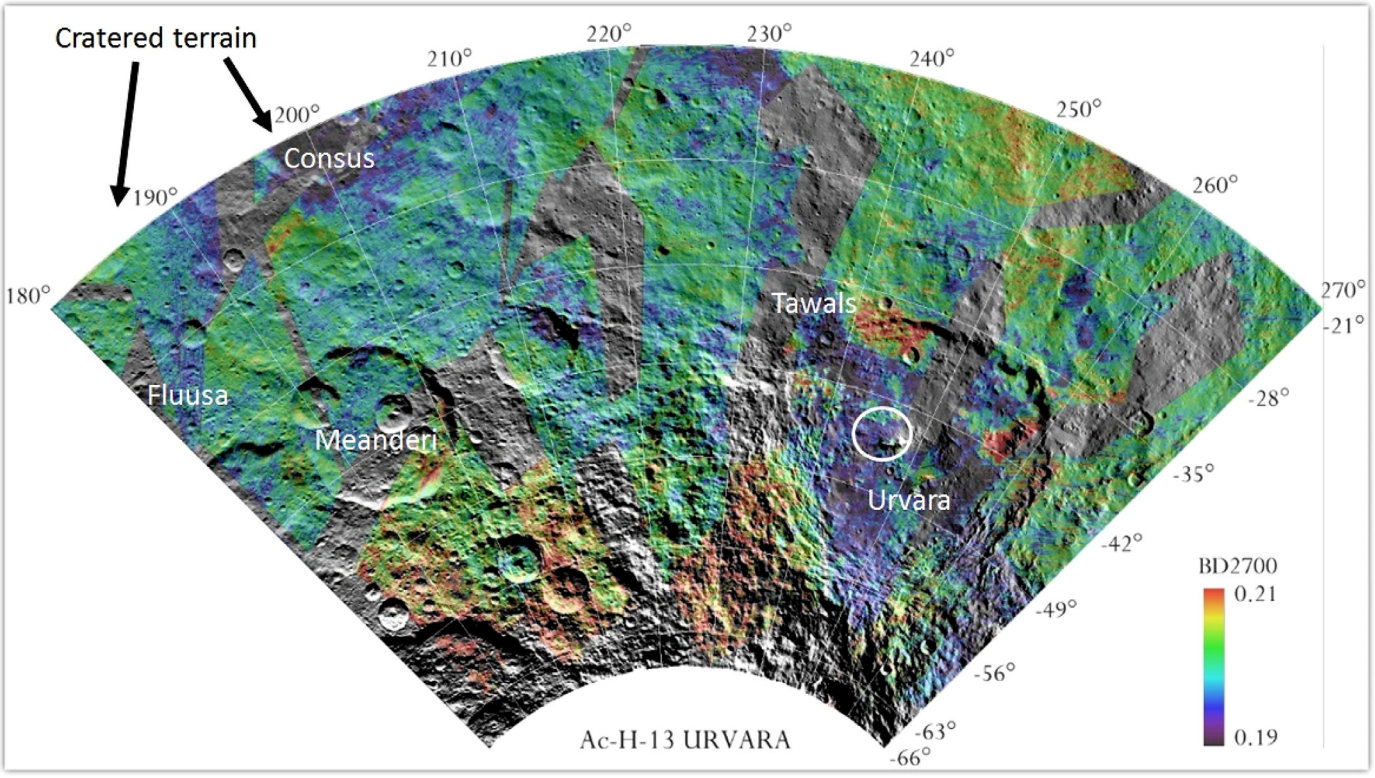

Fig. 3. Map of band depth at 2.7 μm of the Urvara quadrangle, superimposed on the Framing Camera (FC) mosaic with a transparence of 25%. Gray indicates no VIR coverage or excluded data. The white circle encloses the Urvara peak.

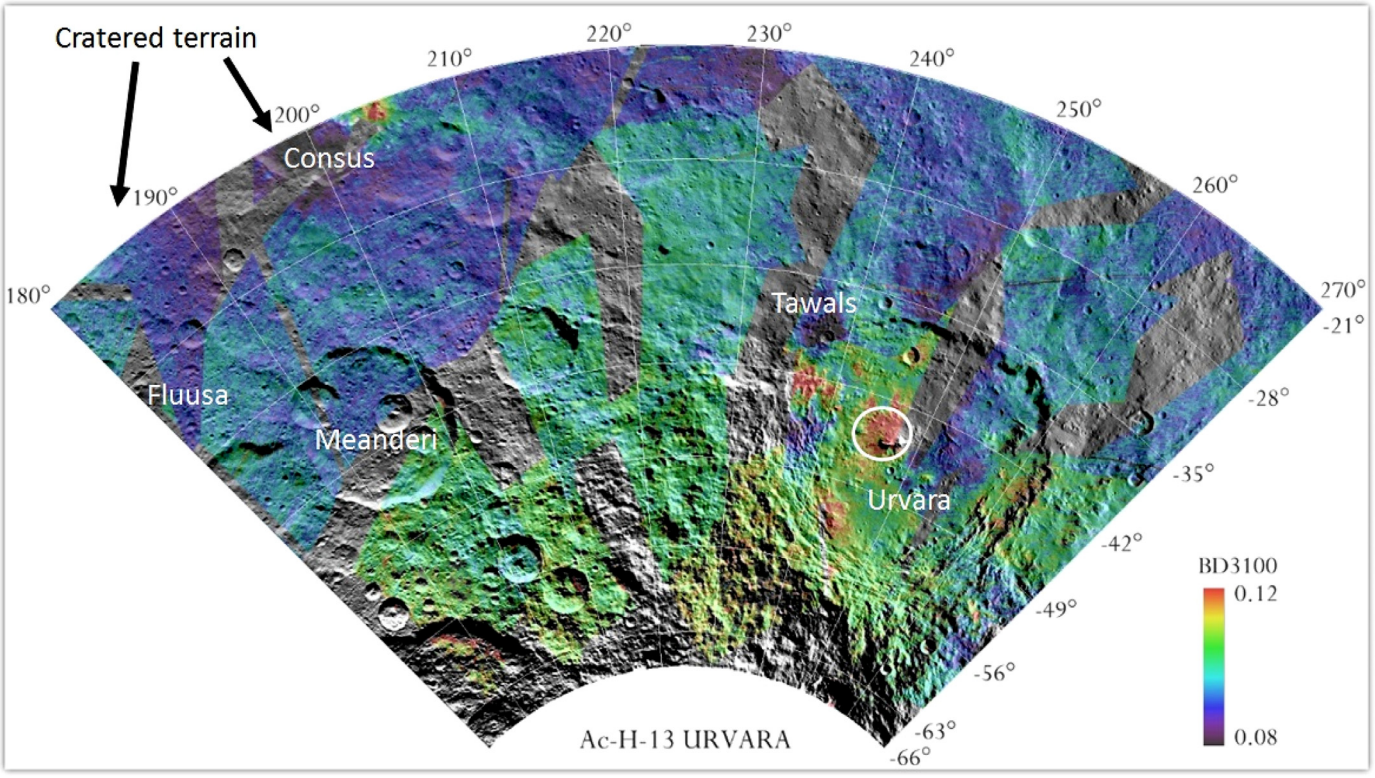

Fig. 4. Map of band depth at 3.1 μm of the Urvara quadrangle, superimposed on the Framing Camera (FC) mosaic with a transparence of 25%. Gray indicates no VIR coverage or excluded data. The white circle encloses the Urvara peak.

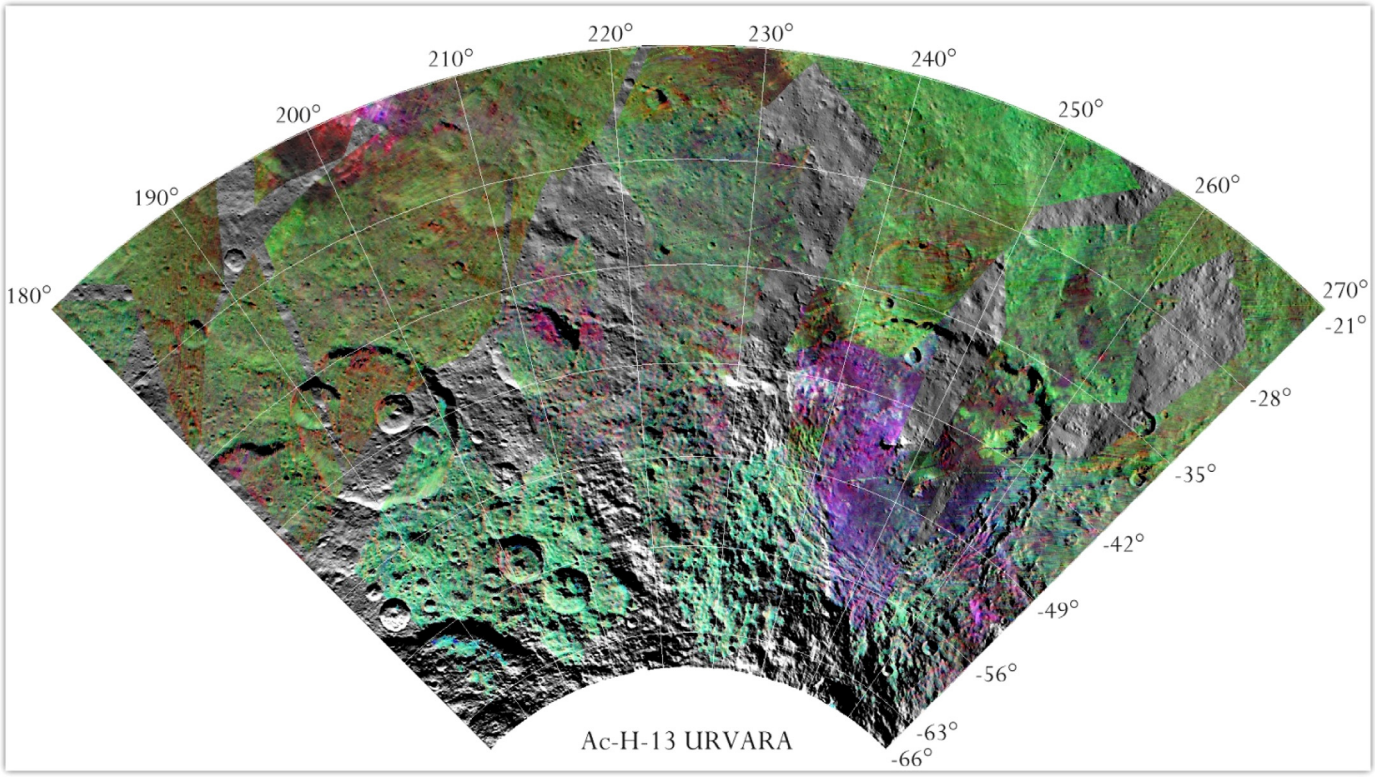

Fig. 5. RGB color map of the Urvara quadrangle, where red, green and blue correspond to reflectance at 1.2 μm, band depth at 2.7 μm and band depth at 3.1 μm, respectively. (For interpretation of the references to color in this figure legend, the reader is referred to the web version of this article.)

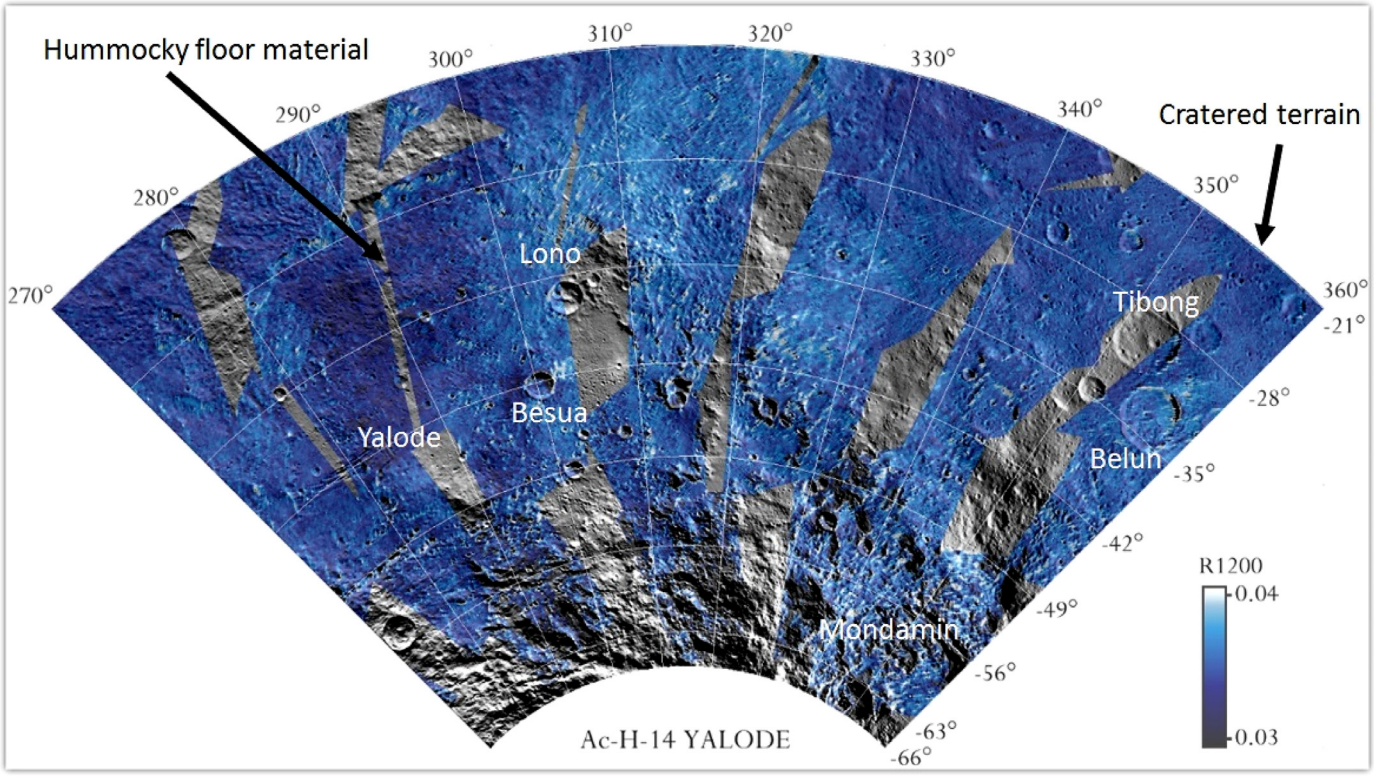

Fig. 6. Map of 1.2 μm reflectance at 30° phase of the Yalode quadrangle, superimposed on the Framing Camera (FC) mosaic with a transparence of 25%. Gray indicates no VIR coverage or excluded data.

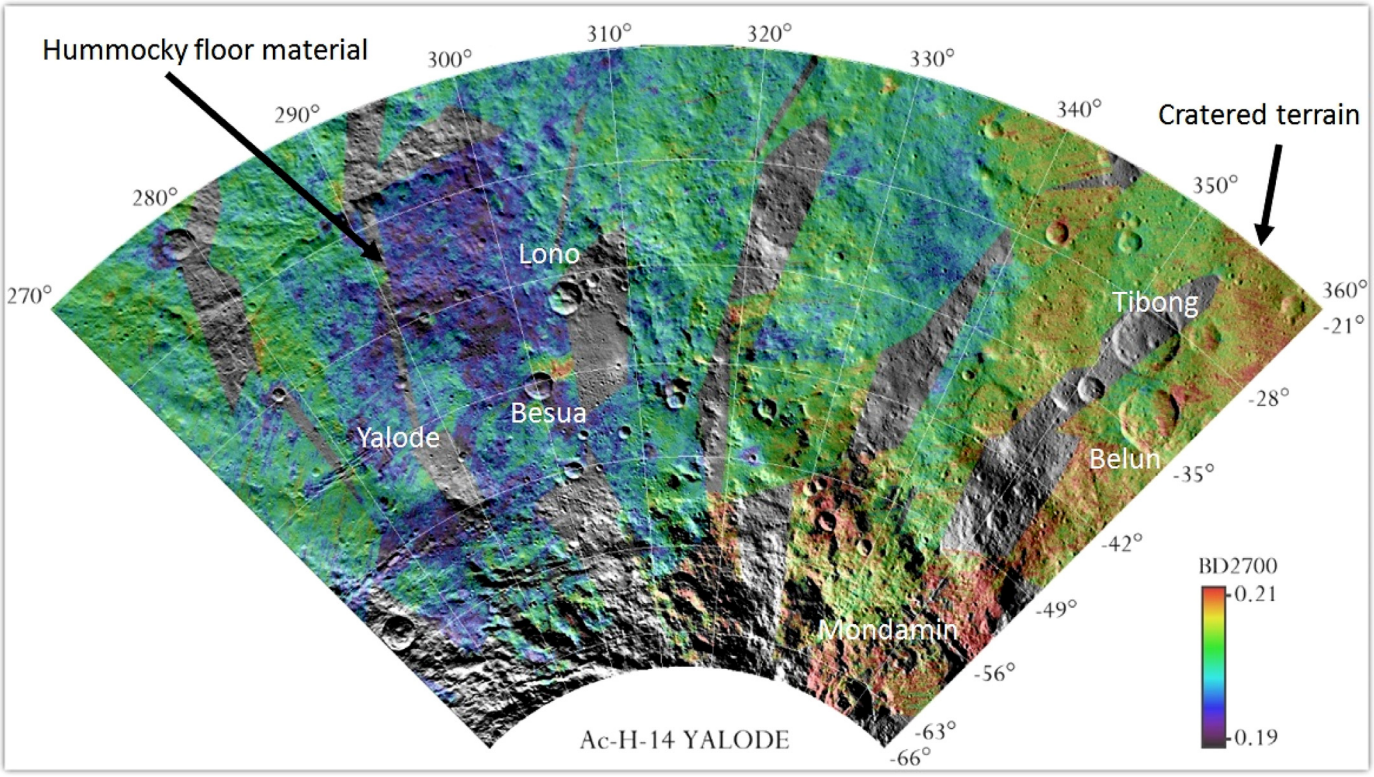

Fig. 7. Map of band depth at 2.7 μm of the Yalode quadrangle, superimposed on the Framing Camera (FC) mosaic with a transparence of 25%. Gray indicates no VIR coverage or excluded data.

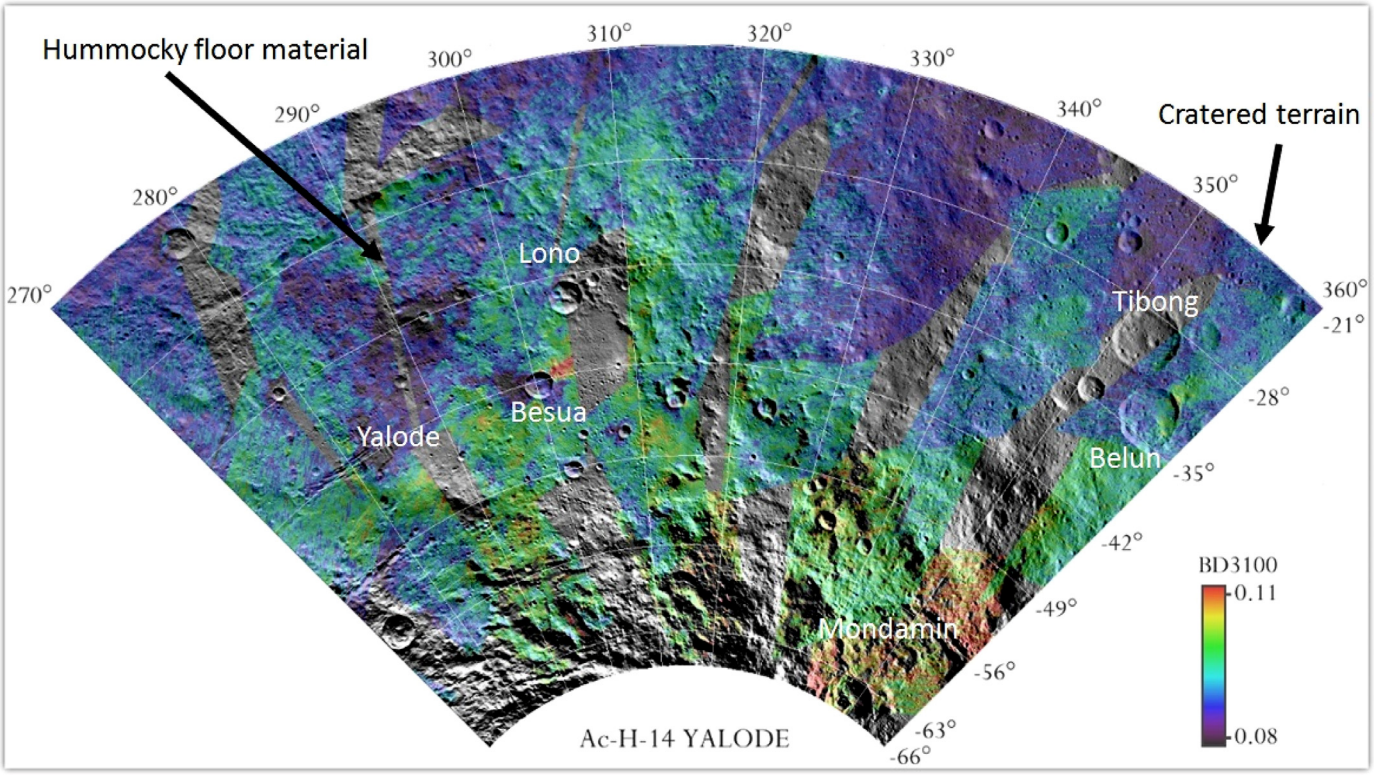

Fig. 8. Map of band depth at 3.1 μm of the Yalode quadrangle, superimposed on the Framing Camera (FC) mosaic with a transparence of 25%. Gray indicates no VIR coverage or excluded data.

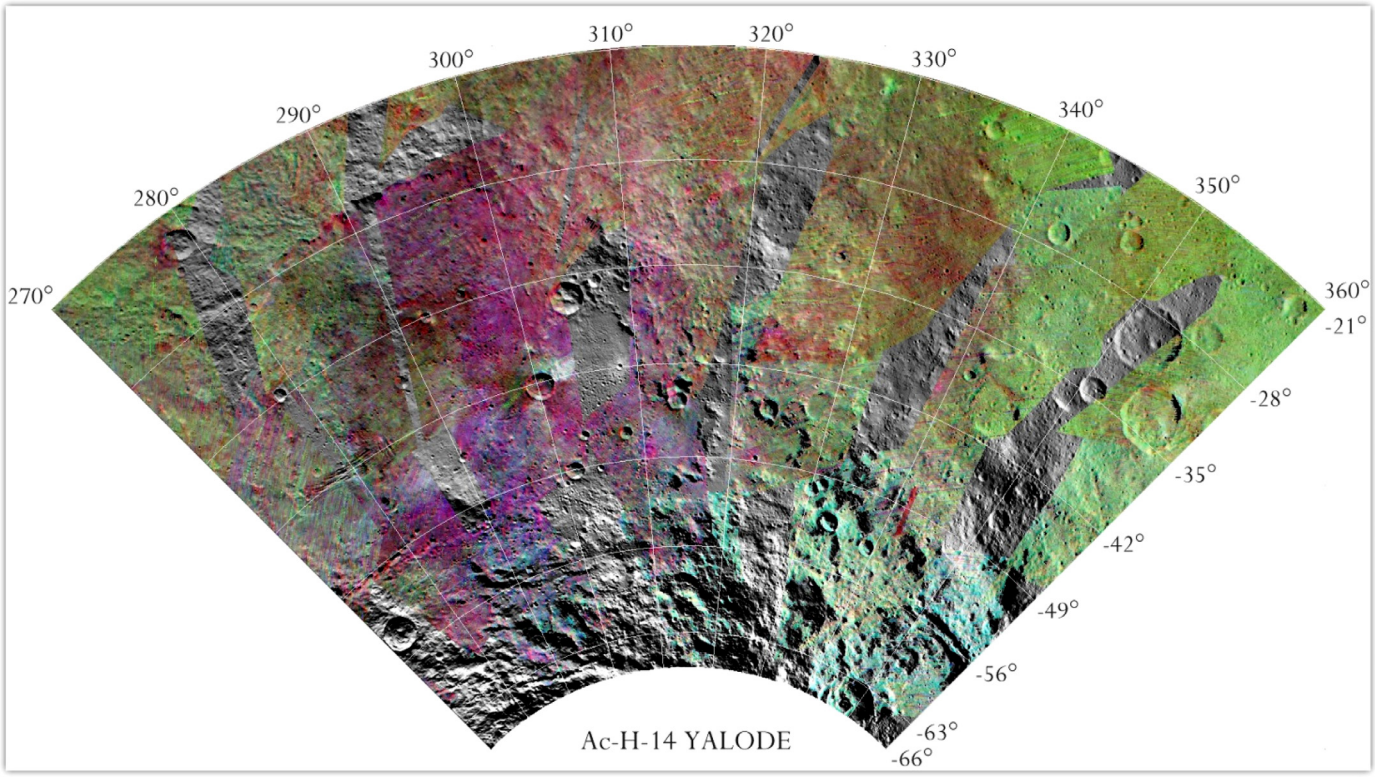

Fig. 9. RGB color map of the Yalode quadrangle, where red, green and blue correspond to reflectance at 1.2 μm, band depth at 2.7 μm and band depth at 3.1 μm, respectively. (For interpretation of the references to color in this figure legend, the reader is referred to the web version of this article.)

observed also at equatorial latitudes with band depths decreasing from Kerwan (Palomba et al., 2017b; longitudes 72–144°E) to Occator quadrangle (Longobardo et al., 2017; longitudes 216–288°E). While at equatorial latitudes, the band depth change corresponds to a topographic variation (Carrozzo et al., 2017a), observed in the Nawish quadrangle (longitudes 144–216°E), there is no abrupt topographic change at southern latitudes, suggesting that the dichotomy is due to a different Mg- and ammoniated phyllosilicates abundance, regardless of altitude.

The slight reflectance variations within each quadrangle are not correlated with particular features. However, many bright spots, mostly associated to craters, are observed at small scale (i.e. LAMO resolution) and are discussed in Section 5.7.

The distribution of band depths in the Urvara quadrangle is also uncorrelated with geology, with cratered terrains not recognizable from spectral maps.

On the contrary, large-scale geological units emerge from spectral maps of the Yalode quadrangle. 2.7 μm and 3.1 μm bands are deeper in correspondence with old, cratered terrain, indicating that the impact generating Yalode probably caused a phyllosilicates depletion. An alternative explanation would be that the grain size changed as a consequence of the impact. However, we would expect that grain size homogenizes with time and Ceres craters younger than Yalode do not show grain size differences with respect to surroundings (Stephan et al., 2017), therefore this hypothesis is unlikely.

Hummocky floor material is another geological unit detectable in spectral maps. It is observed in the Yalode and Besua craters and is characterized by a lower albedo and shallower bands. This behavior could be related to the change of roughness in these terrains.

5. Main features

The geological and mineralogical features are analyzed in this section. However, a detailed mineralogical analysis of several craters (Lono, Mandanin, Tobung, Fluusa) is not possible due to the lack of VIR coverage.

5.1. Urvara

Urvara crater (46°S–149°E, 170 km diameter) dominates the morphology of the region. Looking at the morphology of the terrain, this crater has a north-south dichotomy with the north dominated by smooth material while the south is made by rough surfaces (Crown et al., 2017).

Spectral parameters, however, do not follow this behavior. The albedo of the floor is brighter than the average of the region. Such a high albedo region, however, is not correlated with the geological units. The phyllosilicates and ammonium bands, respectively at 2.7 and 3.1 μm, are generally correlated with the east side having lower values than the west, although there is a positive anomaly in the ammonium content (higher values of 3.1 μm band) on the peak of the crater (Fig. 10).

The peak of Urvara is, in fact, the region with the higher content of ammonium within the entire surface of Ceres. It is interesting to note that Urvara is the crater that hosts the lowest topographic terrain on Ceres (Park et al., 2016), and that might be correlated with the concentration of ammoniated material, although this correlation is not valid everywhere on Ceres. In analogy with other craters (e.g., Raponi et al., 2017a; Singh et al., 2017; Tosi et al., 2017; Zambon et al., 2017), the ejecta have shallower bands, particularly in the north-east direction.

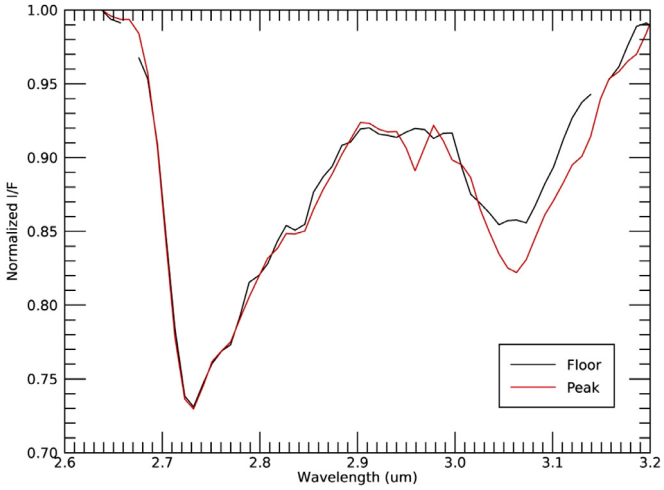

Fig. 10. Continuum-normalized spectra of the Urvara floor (black) and peak (red) in the 2.6–3.2 μm spectral range. (For interpretation of the references to color in this figure legend, the reader is referred to the web version of this article.)

5.2. Yalode

The large Yalode basin, centered at 42.3°S 293.6°E, does not show distinctive spectral signatures with respect to surroundings. This is because of its old age (1.1 Ga, Crown et al., 2017), and therefore a strong degradation and consequent mixing occurred in this region. The only mineralogical variations are found in correspondence of the hummocky area of the floor, characterized by a different roughness as discussed in Section 4, and of the internal, small Besua crater, discussed in sub-section 5.5.

Yalode is, on average, darker than Urvara. However, its ejecta, covering the southern region of the Occator quadrangle, show the opposite trend being brighter than the Urvara ones (Longobardo et al., 2017). Reflectance differences are, however, small (reflectance is always comprised between 0.03 and 0.04), and are not associated to differences in band depth (except for the ammonium excess in the Urvara floor). A plausible explanation is that ejecta reflected the original spectral properties of the subsurface of the two regions, whereas the floors were affected by events during and post-impact (e.g., formation of central peak or hummocky terrains) which changed slightly their composition and physical roughness.

5.3. Consus

The Consus crater is located at 21°S 200°E between the Urvara and Nawish quadrangles (Carrozzo et al., 2017b). It is characterized by a low albedo and shallow bands with respect to surroundings. This could indicate both a larger abundance of dark material and coarser grains. The latter hypothesis is however unlikely, since grain size variations are observed on Ceres on young features (Stephan et al., 2017), whereas Consus is in the oldest region of the quadrangle.

Consus also hosts an internal crater (21°S 204°E), showing opposite behavior (it can be observed in the northern boundary of Figs. 2–4), i.e., larger reflectance and deeper bands. However, it is a different geological unit and is characterized by the occurrence of a carbonate deposit (Carrozzo et al., 2017b), changing its spectral properties.

5.4. Tawals

The Tawals crater (39.1°S, 238°E) is located in the northern rim of the Urvara crater. As Consus, it shows both low albedo and shallow bands. This is common behavior among Ceres craters younger than 500 Ma and is generally ascribed to formation of coarse grain-sized material following the impact (Stephan et al., 2017). As well, we could not discard a larger abundance of dark material in this crater.

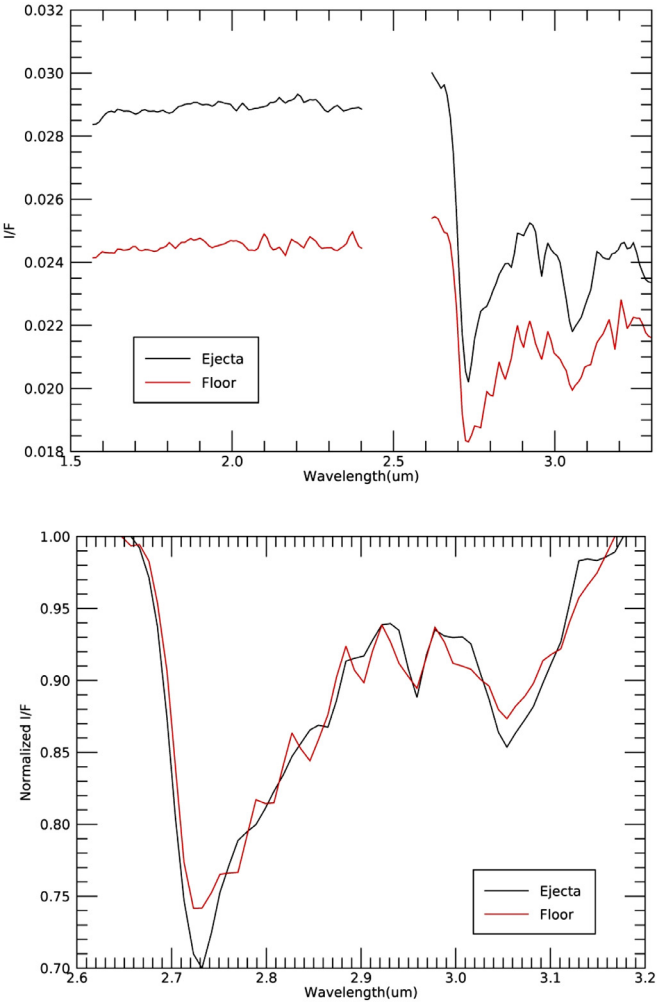

Fig. 11. I/F (top) and continuum-normalized (bottom) spectra of Besua floor and ejecta.

5.5. Besua

The Besua crater (42.4°S, 300.2°E) is located inside the Yalode basin. Its floor and its ejecta are spectrally different: whereas low reflectance and band depths are observed inside the crater, the eastern ejecta are brighter and showing deeper bands (Fig. 11). This is not common behavior among Ceres craters.

The Besua floor is hummocky, and its spectral behavior is similar to hummocky floor material of Yalode, and hence ascribed to a different roughness. The NH4- and OH- rich material in the ejecta may instead reflect the original subsurface composition, in agreement with larger abundance of these compounds predicted in the Ceres subsurface (e.g., Stephan et al., 2017; Carrozzo et al., this issue).

5.6. Meanderi and Belun

Meanderi (40.9°S, 193.7°E) and Belun (33.7°S, 356.3°E) are located in the cratered terrain of the Urvara and Yalode quadrangle, respectively. They are not associated with spectral variations,

Table 1
List of BS located in the Urvara and Yalode quadrangles, with their corresponding coordinates and geomorphological context.

Quadrangle	Latitude	Longitude	Geological feature
Urvara	22.5°S	250.5°E	Crater rim
Urvara	25.5°S	187.3°E	Crater rim
Urvara	36°S	241.5°E	Crater wall
Urvara	41°S	256°E	Crater floor
Urvara	47.5°S	251.7°E	Crater floor
Urvara	51.5°S	191.5°E	Crater wall
Urvara	51.5°S	232.5°E	Crater wall
Urvara	53°S	247.5°E	Crater wall
Urvara	55°S	185°E	Crater rim
Yalode	27°S	310.1°E	Linear feature
Yalode	27°S	342.5°E	Crater wall
Yalode	30.5°S	302.5°E	Crater wall
Yalode	31.5°S	298.5°E	Crater wall
Yalode	31.5°S	305.9°E	Crater rim
Yalode	34°S	301.7°E	Crater wall
Yalode	34.3°S	306°E	Linear feature
Yalode	36.3°S	306.7°E	Linear feature
Yalode	40.5°S	276.5°E	Crater wall
Yalode	42°S	296.4°E	Crater wall
Yalode	43.5°S	297°E	Crater wall
Yalode	48.5°S	298.3°E	Crater wall
Yalode	50.5°S	293.7°E	Crater wall

in agreement with their location in old terrain and with the occurred mixing.

5.7. Bright spots

During the Dawn mission, many "bright spots" (BS) have been detected on Ceres (e.g., Stein et al., 2017). The prototypes are Cerealia and Vinalia Faculae, characterized by a large amount of Na-carbonates (De Sanctis et al., 2016; Raponi et al., 2017a). On the basis of the Occator faculae, such bright areas are probably the result of phenomena like cryovolcanism (Russell et al., 2016; De Sanctis et al., 2016) or hydrothermal activity (Bowling et al., 2016; De Sanctis et al., 2016).

Bright spots have been defined by Palomba et al. (2017a) as groups of pixels having a reflectance at least 30% higher than the average of the corresponding hyperspectral image.

Most of BS of the Urvara and Yalode quadrangles have been detected in LAMO data (spatial resolution of 90–110 m/pixel).

In the Urvara and Yalode quadrangle, nine and thirteen bright spots have been identified, respectively. They are listed in Table 1, in addition to their latitude, longitude and geological context.

On the basis of geomorphological properties, BS can be divided into ejecta, crater-associated features (i.e., rim, floor and wall), and linear features. Most BS of Urvara and Yalode quadrangle are related to impact craters.

The mineralogical analysis of these BS is based on band depths of 2.7 and 3.1 μm spectral features. A scatterplot of 2.7 vs 3.1 μm band depths of BS located in the Urvara (green diamonds) and Yalode (blue diamonds) quadrangle is shown in Fig. 12**.** A moderate correlation between band depths is suggested by the quite high value Pearson coefficient (defined as $\sigma_{FB}/\sigma_F\sigma_B$, being $\sigma_F, \sigma_B$and σ_{FB} the variance of the two sets of parameters and their covariance, respectively, and already used in the spectral analysis of planetary surfaces, e.g., Palomba et al., 2015), i.e. 0.56. This suggests that the occurrence of Mg-phyllosilicates is strictly related to that of ammoniated phyllosilicates, as observed for the entire Ceres surface (Ammannito et al., 2016). According to the definitions by Palomba et al. (2017a), these BS's are "typical BS", i.e., differing from the Ceres average only for the highest reflectance, while the other spectral parameters (such as band depths) are similar. This is in agreement with the overall old age of this Ceres region.

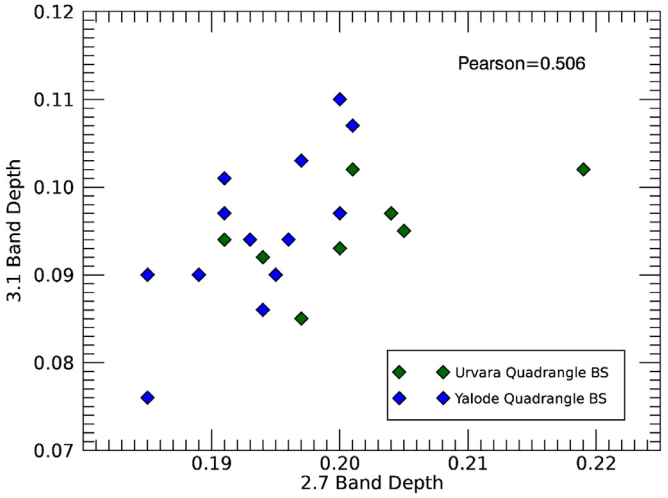

Fig. 12. Scatterplot of 2.7 vs 3.1 μm band depths of BS located in the Urvara (green diamonds) and Yalode (blue diamonds) quadrangle. Spectral parameters are moderately correlated, with a Pearson coefficient value of 0.506. (For interpretation of the references to color in this figure legend, the reader is referred to the web version of this article.)

6. Conclusions

We mapped the distribution of the reflectance at 1.2 μm, band depth at 2.7 μm and band depth at 3.1 μm of the Urvara and Yalode quadrangles, located in the Southern hemisphere of Ceres (from 21°S to 66°S), at longitudes 180–270°E and 270–360°E, respectively.

The two quadrangles are named after their two large impact craters. The spectral and mineralogical properties do not reproduce the geomorphology of these craters, even if two internal units show distinctive spectral signatures. The Urvara crater peak is characterized by the deepest 3.1 μm band of Ceres, reflecting an excess of ammoniated materials. Because Urvara is the lowest topographic terrain of Ceres, this might indicate a larger abundance of these materials in the Ceres subsurface. The hummocky floor of Yalode shows low values of both reflectance and band depths, probably because of different roughness: this behavior is observed also on the hummocky floor of Besua crater.

Decreasing reflectance and band depth in correspondence with Consus and Tawals craters is observed, as in other quadrangles of Ceres (e.g., Stephan et al., 2017), and ascribed to coarser grain size (Tawals) or abundance of dark materials (Consus).

The overall mineralogy of the Urvara-Yalode region is characterized by band depths shallower than the eastern quadrangles at the same latitudes, reflecting the E-W dichotomy of Ceres (Ammannito et al., 2016), and by spectral behaviors which could be explained by the old age of this region, i.e.: a) no spectral parameter variations in correspondence with most craters (e.g., Yalode, Meanderi, Belun); b) occurrence of 22 bright spots having spectral properties similar to the Ceres average, indicating a strong mixing. Mineralogy is uncorrelated with geology in the Urvara quadrangle (a common behavior among asteroids, e.g., Longobardo et al., 2015), whereas in the Yalode quadrangle, band depths are larger in the old, cratered terrain, probably because of phyllosilicate depletion caused by the Yalode impact.

Acknowledgments

VIR is funded by the Italian Space Agency-ASI(ASI-INAF n. I/004/12/0) and was developed under the leadership of INAF-Istituto di Astrofisica e Planetologia Spaziali, Rome-Italy. The instrument was built by Selex-Galileo, Florence-Italy. The authors

acknowledge the support of the Dawn Science, Instrument, and Operations Teams.

We thank the FC team for sharing their images.

David Williams (ASU) and Mario D'Amore (DLR) are thanked for their efforts to review and improve the manuscript.

Sharon Uy (UCLA) is thanked for the manuscript revision.

References

Ammannito, E., et al., 2016. Distribution of phyllosilicates on the surface of Ceres. Science 353, 6303. doi:10.1126/science.aaf4279.

Bowling, T.J., et al., 2016. Impact induced heating of Occator crater on Asteroid 1 Ceres. In: 47th LPSC, 1903, p. 2268.

Carrozzo, F.G., et al., 2016. Artifacts reduction in VIR/Dawn data. Rev. Sci. Instr. 87, 12. doi:10.1063/1.4972256.

Carrozzo, F.G., et al., 2017a. Nature, formation and distribution of Carbonates on Ceres. Sci. Adv. Under Review.

Carrozzo, F.G., et al., 2017b. The mineralogy of the Nawish Quadrangle of Ceres. Icarus submitted to Icarus, this issue.

Ciarniello, M., et al., 2017. Spectrophotometric properties of dwarf planet Ceres from VIR onboard Dawn mission. Astron. Astrophys. 598, A130.

Clark, R.N., Roush, T.L., 1984. Reflectance spectroscopy: quantitative analysis techniques for remote sensing applications. J. Geophys. Res. 89 (B7), 632–6340.

Crown, D., et al., 2017. Geologic mapping of the Urvara and Yalode Quadrangles of Ceres. Icarus. in press doi: 10.1016/j.icarus.2017.08.004.

De Sanctis, M.C., et al., 2011. The VIR spectrometer. Space Sci. Rev. 163, 329–369.

De Sanctis, M.C., et al., 2015. Ammoniated phyllosilicates with a likely outer system origin on (1) Ceres. Nature 528, 241–244.

De Sanctis, M.C., et al., 2016. Bright carbonate deposits as evidence of aqueous alteration on (1) Ceres. Nature 536, 54–57.

De Sanctis, M.C., et al., 2017a. Localized aliphatic organic material on the surface of Ceres. Science 355 (6326), 719–722.

De Sanctis, M.C., et al., 2017b. Ac-H-11 Sintana and Ac-H-12 Toharu quadrangles: assessing the large and small scale heterogeneities of Ceres' surface. Icarus. this issue, in press doi: 10.1016/j.icarus.2017.08.014.

Filacchione, G. and Ammannito, E. 2014. Dawn VIR calibration document Version 2.4, https://sbn.psi.edu/archive/dawn/vir/DWNVVIR_I1B/DOCUMENT/VIR_CALIBRATION/VIR_CALIBRATION_V2_4.PDF.

Hapke, B., 2012. Theory of Reflectance and Emittance Spectroscopy. Cambridge University Press.

Longobardo, A., et al., 2015. Mineralogical and spectral analysis of Vesta's Gegania and Lucaria quadrangles and comparative analysis of their key features. Icarus 259, 72–90.

Longobardo, A., et al., 2017. Photometry of Ceres and Occator faculae as inferred by VIR/Dawn data. Icarus Under Review.

McCord, T.B. and Zambon, F., 2017. The surface composition of Ceres from the Dawn mission, *Icarus*, submitted to Icarus, this issue.

Palomba, E., et al., 2015. Detection of new olivine-rich locations on Vesta. Icarus 258, 120–134.

Palomba, E., et al., 2017a. Compositional differences among Bright Spots on the Ceres surface. Icarus. in press doi: 10.1016/j.icarus.2017.09.020.

Palomba, E., et al., 2017b. Mineralogical mapping of the Kerwan quadrangle on Ceres. Icarus. in press doi: 10.1016/j.icarus.2017.07.021.

Park, R.S., et al., 2016. Gravity Science Investigation of Ceres from Dawn. In: 47th LPSC, 1903, p. 1781.

Prettyman, T.H., et al., 2011. Dawn's Gamma Ray and Neutron Detector. Space Sci. Rev. 163, 371–459.

Raponi, A., et al., 2017a. Mineralogical mapping of Ac-H-2 'Coniraya' quadrangle. Icarus. this issue, in press doi: 10.1016/j.icarus.2017.10.023.

Raponi, A., et al., 2017b. Mineralogy of Occator crater on Ceres. Icarus Under Review.

Russell, C.T., Raymond, C.A., 2011. The Dawn Mission to Vesta and Ceres. Space Sci. Rev. 163 (1-4), 3–23.

Russell, C.T., et al., 2016. Dawn arrives at Ceres: exploration of a small, volatile-rich world. Science 353 (6303), 1008–1010.

Sierks, H., et al., 2011. The Dawn Framing Camera. Space Sci. Rev. 163, 263–327.

Singh, S., et al., 2017. Mineralogy mapping of the Ac-H-5 Fejokoo quadrangle of Ceres. Icarus Under Review.

Stein, N., et al., 2017. Characteristic, formation and evolution of faculae (bright spots) on Ceres. Icarus. in press doi: 10.1016/j.icarus.2017.10.014.

Stephan, K., et al., 2017. Ceres' craters – relationships between surface composition and geology. Icarus. this issue, in press doi: 10.1016/j.icarus.2017.10.013.

Tosi, F., et al., 2017. Mineralogical analysis of the Ac-H-6 Haulani quadrangle of the dwarf planet Ceres. Icarus. in press doi: 10.1016/j.icarus.2017.08.012.

Williams, D., et al., 2017a. Introduction: The geologic mapping of Ceres. Icarus. in press doi: 10.1016/j.icarus.2017.05.004.

Williams, D., et al., 2017b. The geology of the Kerwan quadrangle of dwarf planet Ceres: Investigating Ceres' oldest impact basin. Icarus. in press doi: 10.1016/j.icarus.2017.08.015.

Zambon, F. et al., 2017. *Mineralogical analysis of Quadrangle Ac-H-10 Rongo on the Dwarf Planet Ceres*, in press, doi:10.1016/j.icarus.2017.09.021.